

Same Prompt, Different Answer: Exposing the Reproducibility Illusion in Large Language Model APIs

Lucas Rover^{1*}[†], Eduardo Tadeu Bacalhau², Anibal Tavares de Azevedo³, Yara de Souza Tadano¹

¹*Graduate Program in Mechanical Engineering, Federal University of Technology — Paraná (UTFPR), Ponta Grossa, Paraná, Brazil.

²Research Group of Technology Applied to Optimization (GTAO), Federal University of Paraná (UFPR), Curitiba, Paraná, Brazil.

³School of Applied Sciences (FCA), University of Campinas (Unicamp), Limeira, São Paulo, Brazil.

*Corresponding author(s). E-mail(s): lucasrover@utfpr.edu.br;

[†]Corresponding author.

Abstract

The same prompt sent twice to a large language model API under documented “deterministic” settings can return different answers, yet this variation is invisible to users. Here we report 4,104 controlled experiments across eight models and five API providers showing that, under temperature-zero greedy decoding with fixed seeds, API-served models reproduce their own outputs only 22.1% of the time (exact match rate), while locally deployed models achieve 95.6%, a gap exceeding four-fold. The non-determinism persists in multi-turn and retrieval-augmented generation workflows, where one model produces zero exact matches across 50 runs, yet remains hidden because outputs are semantically equivalent (BERTScore F1 > 0.97). A quasi-isolation experiment identifies production infrastructure complexity, rather than cloud deployment itself, as the driver. We provide a lightweight provenance protocol (<1% overhead) that makes this variation detectable, raising a reliability concern for the growing use of LLMs in medicine, physical sciences, and automated data analysis.

Keywords: Reproducibility, Large language models, Non-determinism, Provenance, API inference

1 Large language models (LLMs) are rapidly becoming standard research instruments.
2 They encode clinical knowledge[1], assist diagnostic workflows[2], accelerate liter-
3 ature review and data extraction[26], and are increasingly integrated into peer
4 review at scale[3]. A growing body of work deploys LLMs as evaluators of human
5 communication[13], as psychometric assessment tools[14], and as components of multi-
6 agent scientific pipelines[4]. When researchers use API-based models, they trust that
7 identical configurations will yield identical outputs. API documentation reinforces this
8 trust by offering a temperature parameter set to zero for “deterministic” behavior, a
9 setting that should collapse the output probability distribution to a single token at
10 each step. But this is an illusion.

11 The broader reproducibility crisis in science is well documented: over 70% of
12 researchers have failed to reproduce another scientist’s experiment[21], and the prob-
13 lem is acute in AI, where only 6% of papers provide sufficient information for
14 reproduction[23]. The field faces its own “reproducibility crisis”[22], with growing
15 concerns that AI may worsen the problem across disciplines[24]. Data leakage alone
16 has been documented across 17 machine learning subfields[25], and leading AI jour-
17 nals have begun adopting structured reproducibility mechanisms in response[19]. Yet
18 despite this attention to training-time reproducibility, the reproducibility of *inference*,
19 the actual deployment of models to generate outputs, remains largely unexamined.
20 This gap matters because inference is the stage at which LLMs interact with research
21 data and produce the outputs that enter scientific records, policy documents, and clin-
22 ical workflows. Existing experiment-tracking tools such as MLflow[50] were designed
23 for training pipelines and numerical metrics, not for inference-time text-generation
24 provenance.

25 We conducted 4,104 controlled experiments across eight models and five indepen-
26 dent API providers and found that even under temperature = 0 with fixed random
27 seeds, API-served models reproduce their own outputs only 22.1% of the time, while
28 locally deployed open-weight models achieve 95.6% exact reproducibility, a gap exceed-
29 ing four-fold (95% bootstrap CI for the ratio: 2.48–3.61×). This non-determinism is
30 invisible to users: outputs are semantically equivalent (BERTScore F1 > 0.97) but
31 textually different, meaning researchers cannot detect the variation by reading out-
32 puts. The phenomenon is not confined to single queries. As LLMs move into agentic
33 pipelines that design experiments and generate hypotheses[4], this hidden variation
34 compounds at every step. Recent editorials have underscored the urgency of trans-
35 parency in multi-agent AI systems[5], yet the baseline reproducibility of the individual
36 API calls has never been systematically quantified.

37 Here, we make four contributions. First, we reveal and quantify hidden non-
38 determinism across all five major API providers tested (OpenAI, Anthropic, Google,
39 DeepSeek, Perplexity), showing that it is a general property of cloud-served LLM APIs
40 rather than a provider-specific anomaly. Second, we show that this non-determinism
41 persists and amplifies in multi-turn and retrieval-augmented generation (RAG) work-
42 flows, where Claude Sonnet 4.5 produces zero exact matches across 50 RAG runs.
43 Third, we demonstrate that cloud deployment *per se* does not cause non-determinism:
44 the same LLaMA 3 8B architecture served via Together AI’s cloud endpoint achieves
45 near-local exact match rates, implicating production-infrastructure complexity (tensor

46 parallelism, speculative decoding, dynamic batching) rather than the cloud medium.
47 Fourth, we provide a lightweight provenance protocol grounded in W3C PROV[6],
48 extending Model Cards[17] and Datasheets[18] to the inference layer, that adds
49 less than 1% overhead and makes this invisible variation visible, auditable, and
50 attributable.

51 Results

52 API-based models fail to reproduce outputs under 53 deterministic settings

54 We evaluated eight models across two core tasks, structured extraction (JSON output)
55 and scientific summarization (free text), under greedy decoding (temperature = 0)
56 with fixed random seeds, the configuration that API documentation presents as
57 deterministic. The results reveal a stark divide (Table 1, Fig. 1).

58 Locally deployed models achieve near-perfect to perfect bitwise reproducibility.
59 Gemma 2 9B produces exact match rate (EMR) = 1.000 [1.00, 1.00] across all tasks
60 and conditions: every output is character-for-character identical across five repeti-
61 tions, confirmed by SHA-256 hash comparison. LLaMA 3 8B attains EMR = 0.987
62 [0.96, 1.00] for structured extraction and 0.947 [0.89, 0.99] for summarization; Mistral
63 7B achieves 0.960 [0.88, 1.00] and 0.840 [0.72, 0.96], respectively. The minor devia-
64 tions in LLaMA 3 and Mistral are attributable to a cold-start effect: post-hoc analysis
65 reveals that in all seven non-unanimous abstract groups, the first repetition was the
66 sole outlier, likely due to GPU cache state initialization on the first forward pass. Dis-
67 carding a single warm-up inference yields EMR = 1.000 for both models (Extended
68 Data Table 5).

69 API-served models tell a starkly different story. Under the same greedy decod-
70 ing with fixed seeds, GPT-4 achieves EMR = 0.443 [0.32, 0.57] for extraction and
71 0.230 [0.16, 0.30] for summarization. Claude Sonnet 4.5 achieves 0.190 [0.05, 0.40]
72 and 0.020 [0.00, 0.05], respectively; across 50 pairwise comparisons, effectively no
73 two summarization outputs were character-identical. Perplexity Sonar falls further to
74 EMR = 0.100 for extraction and 0.010 for summarization. The overall local aver-
75 age EMR is 0.956 versus 0.221 for API models, meaning that fewer than one in four
76 API output pairs are identical under conditions documented as deterministic. This
77 gap survives Holm–Bonferroni correction across 68 hypothesis tests (51 significant at
78 $\alpha = 0.05$; Supplementary Section S9) and is confirmed by large Cliff’s delta effect
79 sizes ($\delta = 0.784\text{--}0.896$), paired t -test (Cohen’s $d > 1.6$), and a balanced 10-abstract
80 subsample analysis that controls for sample-size differences between models (local
81 EMR = 0.953 vs. API EMR = 0.304, $3.1 \times$ gap; Extended Data Table 4). A chat-format
82 control experiment (200 runs) confirmed that the prompt format (completion versus
83 chat API) does not contribute to the observed variation (Supplementary Section S7).

84 Non-determinism varies substantially across providers

85 The five API providers span a wide reproducibility range, with an 80-fold differ-
86 ence between the most and least reproducible (Fig. 1). DeepSeek Chat achieves

87 the highest API reproducibility (EMR = 0.800 for extraction, 0.760 for summarization), approaching local-model performance. GPT-4 occupies an intermediate
88 position (EMR = 0.443 for extraction, 0.230 for summarization), with the extraction–
89 summarization gap suggesting that task output structure mediates reproducibility, as
90 JSON-constrained outputs leave less room for lexical variation than free-text sum-
91 marizations. Claude Sonnet 4.5 (0.190/0.020) and Perplexity Sonar (0.100/0.010) occupy
92 the low end, while Gemini 2.5 Pro (evaluated on multi-turn and RAG tasks only)
93 achieves EMR = 0.010–0.070.

94 This variation is notable because all providers expose the same user-facing “deter-
95 ministic” parameters (temperature zero, fixed seed where supported). The differences
96 therefore reflect production serving infrastructure invisible to users, consistent with
97 editorial calls for explicit model version tracking and prompt disclosure[7]. Structured
98 JSON extraction constrains the output space more tightly than free-text sum-
99 marization, leaving fewer viable token sequences and less opportunity for divergence.
100 This task-dependence suggests that open-ended generation tasks (creative writing,
101 hypothesis formulation) will likely exhibit even larger variation.

102 Perplexity Sonar’s particularly low reproducibility reflects its search-augmented
103 architecture, where real-time web retrieval introduces an additional source of varia-
104 tion that compounds model-internal non-determinism. This observation is particularly
105 relevant as retrieval-augmented approaches become standard in scientific applica-
106 tions: the combination of non-deterministic generation with variable retrieval creates
107 a multiplicative reproducibility challenge that researchers must account for.

109 **Cloud deployment does not preclude reproducibility**

110 A natural hypothesis is that cloud deployment itself (network latency, load balancing,
111 shared hardware) causes the non-determinism. To test this, we designed a quasi-
112 isolation probe: we evaluated the same LLaMA 3 8B architecture served via Together
113 AI’s cloud endpoint (INT4 quantisation) under identical prompts, seeds, and temper-
114 ature as the local deployment. If cloud hosting were the driver, this deployment should
115 exhibit API-like non-determinism.

116 It does not. The cloud-served LLaMA 3 achieves EMR = 1.000 [1.00, 1.00] for
117 extraction and 0.880 [0.70, 1.00] for summarization, nearly identical to the local deploy-
118 ment on the same 10-abstract subset (EMR = 1.000 and 0.920, respectively; 95%
119 bootstrap confidence intervals overlap). This provides evidence that cloud deployment
120 *per se* does not cause non-determinism. The variability observed in GPT-4, Claude,
121 and Gemini is instead consistent with the complexity of their production serving
122 infrastructure.

123 Six well-documented mechanisms in distributed GPU inference can indepen-
124 dently produce non-deterministic outputs even under greedy decoding (see Meth-
125 ods): non-associative floating-point arithmetic[15], mixed-precision accumulation
126 in BF16/FP16[11], multi-GPU tensor parallelism[8], FlashAttention kernel non-
127 determinism[16], dynamic batching with continuous request scheduling[10], and
128 speculative decoding[9]. Our single-GPU local deployment eliminates mechanisms 3–
129 6, and GGML Q4 integer arithmetic mitigates mechanism 2, explaining near-perfect

130 local reproducibility as a predicted consequence of the simpler execution environment.
131 The Together AI result confirms that this is not an inherent limitation of cloud
132 deployment: a well-controlled cloud serving environment can achieve near-local repro-
133 ductibility. Deterministic execution modes are technically feasible, though they may
134 entail performance trade-offs that current serving architectures prioritize differently.

135 **Complex workflows amplify the reproducibility gap**

136 Modern LLM applications rarely consist of single API calls. Multi-turn refinement
137 dialogues and retrieval-augmented generation (RAG) pipelines are increasingly com-
138 mon in research workflows. To assess whether non-determinism compounds in these
139 settings, we evaluated five models on a three-turn refinement task (extract, receive
140 feedback, refine) and a RAG extraction task (extract structured fields from an abstract
141 with a prepended retrieved context passage).

142 Local models maintain high reproducibility even under these more complex regimes
143 (Fig. 2). Gemma 2 9B and Mistral 7B achieve perfect EMR = 1.000 for both multi-
144 turn and RAG. LLaMA 3 8B shows EMR = 0.880 [0.76, 1.00] for multi-turn and 0.960
145 [0.88, 1.00] for RAG, slightly lower than single-turn, consistent with error propagation
146 across dialogue turns where each response conditions the next.

147 Both API models exhibit near-zero reproducibility. Claude Sonnet 4.5 achieves
148 EMR = 0.040 [0.00, 0.08] for multi-turn and 0.000 [0.00, 0.00] for RAG. Across 50 runs,
149 not a single pair of RAG outputs was character-identical, with a mean normalized
150 edit distance (NED) of 0.256. Gemini 2.5 Pro, despite supporting a seed parameter,
151 achieves EMR = 0.010 [0.00, 0.03] for multi-turn and 0.070 [0.02, 0.13] for RAG. The
152 convergence of two independent API providers, using different model architectures and
153 serving stacks, on near-zero multi-turn reproducibility indicates that this is a general
154 property of cloud-served inference for complex interaction regimes. This is concern-
155 ing for agentic AI workflows, where LLMs are chained across multiple steps. If each
156 step introduces independent non-deterministic variation, end-to-end reproducibility
157 becomes unattainable without explicit provenance tracking at every node.

158 **Outputs diverge textually but not semantically**

159 If API outputs varied randomly, producing nonsensical or contradictory results, the
160 problem would be easy to detect. Instead, our multi-level metric analysis reveals a sub-
161 tler pattern (Fig. 3). Across all models and conditions, BERTScore F1 remains above
162 0.97 even when EMR approaches zero. ROUGE-L scores similarly remain high (>0.85
163 for all models), confirming substantial token-level overlap. This three-level dissocia-
164 tion (low bitwise identity, moderate surface divergence, high semantic preservation)
165 defines “hidden” non-determinism: same meaning, different words. A researcher read-
166 ing two outputs from the same prompt would judge them equivalent; only systematic
167 comparison reveals that they are textually distinct.

168 Yet this hidden variation has practical consequences that extend beyond surface-
169 level differences. A field-level divergence analysis of GPT-4 structured extraction
170 outputs reveals that 100% of non-identical output pairs (24 of 30 abstract groups) dif-
171 fer in at least one conclusion-relevant field: objective, method, or key result (Extended

172 Data Table 7). The `key_result` field diverges in 67% of groups, and `method` in 57%,
173 meaning the textual variation is not limited to formatting or filler words but affects
174 the substantive content that researchers would use for downstream analysis. For
175 automated evidence synthesis pipelines, where outputs are parsed programmatically
176 rather than read by humans, even minor lexical differences can propagate to different
177 extracted values, different aggregated statistics, and ultimately different conclusions.

178 The implications extend beyond individual studies. Recent work has shown that
179 LLMs used as evaluators of empathic communication are sensitive to subtle input
180 variations[13], and psychometric assessments of LLM behavior reveal consistency
181 patterns that depend on model architecture and fine-tuning approach[14]. Non-
182 determinism is therefore not a technical curiosity but a property that interacts with
183 how LLMs are deployed as measurement instruments, one that current evaluation
184 frameworks do not account for. For the growing body of work that uses LLMs as anno-
185 tators, evaluators, or data extractors, our results indicate that the “instrument” itself
186 introduces measurement noise that is uncharacterized and unreported in standard
187 methodology sections.

188 Temperature paradox: greedy decoding is not greedy for APIs

189 Temperature is the primary user-controllable parameter governing output variability.
190 For local models, it behaves as theory predicts: under the temperature sweep (Fig. 4),
191 local models show a clean monotonic decline from near-perfect EMR at $t = 0$ to
192 $\text{EMR} \approx 0$ at $t = 0.7$. This confirms that local greedy decoding is truly greedy, collapsing
193 the output distribution to a single deterministic sequence. API models, however, start
194 from an already-low baseline at $t = 0$ and show a more complex pattern that violates
195 the expected monotonicity.

196 Claude Sonnet 4.5 exhibits a non-monotonic response: extraction EMR *increases*
197 from 0.067 at $t = 0.0$ to 0.700 at $t = 0.3$ before declining to 0.133 at $t = 0.7$. This
198 counterintuitive result, where adding randomness *improves* reproducibility, suggests
199 that Anthropic’s $t = 0$ decoding path exposes more infrastructure-level stochasticity
200 than a small positive temperature that activates a more stable sampling pathway.
201 GPT-4 shows a less dramatic but qualitatively similar pattern: the difference between
202 $t = 0$ and $t = 0.3$ is smaller for API models than for local models, because the
203 API baseline is already far from deterministic. At $t = 0.7$, local and API models
204 converge toward uniformly low EMR, but through different trajectories: local models
205 decline monotonically from near-1.0, while API models follow a flatter curve from an
206 already-degraded baseline.

207 This temperature paradox has important practical implications. Researchers who
208 set temperature to zero expecting deterministic outputs are, for API models, not
209 achieving the greedy decoding they intend. The temperature–reproducibility relation-
210 ship for API models depends on provider-specific implementation details that are
211 opaque to users and undocumented in API references[12], making it impossible for
212 researchers to predict or control the degree of non-determinism in their experiments
213 without empirical measurement.

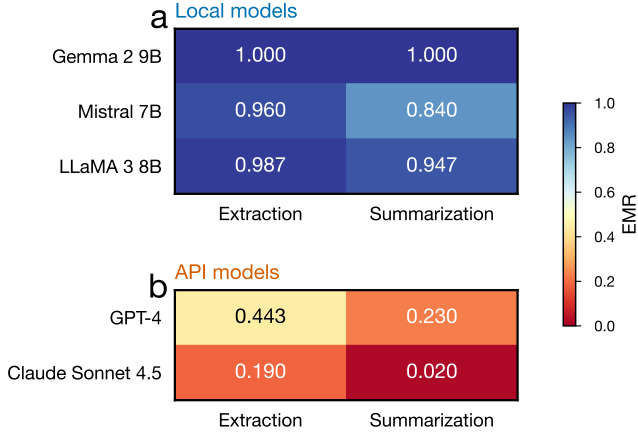


Fig. 1 Exact match rates under greedy decoding reveal a four-fold local–API gap. Heatmap of EMR for eight model deployments across extraction and summarization tasks under temperature = 0. Local models (top; blue) achieve EMR ≥ 0.840 , with Gemma 2 9B at a perfect 1.000. API-served models (bottom; red) range from 0.800 (DeepSeek) to 0.010 (Perplexity). All values are computed under each model’s representative greedy condition (C1 for local models and Claude; C2 for GPT-4; see Methods).

Table 1 Exact match rate under greedy decoding with 95% bootstrap confidence intervals. For local models, values reflect the fixed-seed condition (C1); for GPT-4, the variable-seed greedy condition (C2); for Claude, C1 (no seed parameter supported). Bootstrap: 10,000 resamples, percentile method. n = number of abstracts per group.

Model	Deployment	n	Extraction EMR	Summarisation EMR
Gemma 2 9B	Local	10	1.000 [1.00, 1.00]	1.000 [1.00, 1.00]
LLaMA 3 8B	Local	30	0.987 [0.96, 1.00]	0.947 [0.89, 0.99]
Mistral 7B	Local	10	0.960 [0.88, 1.00]	0.840 [0.72, 0.96]
DeepSeek Chat	API	10	0.800	0.760
GPT-4	API	30	0.443 [0.32, 0.57]	0.230 [0.16, 0.30]
Claude Sonnet 4.5	API	10	0.190 [0.05, 0.40]	0.020 [0.00, 0.05]
Perplexity Sonar	API	10	0.100	0.010
<i>Local average</i>			0.982	0.929
<i>API average</i>			0.383	0.255

Discussion

Our findings reveal a pervasive and previously invisible reproducibility gap in LLM-based research. Under the settings that API documentation presents as deterministic (temperature zero, fixed seed), API-served models fail to reproduce their own outputs approximately four out of five times. This gap persists across five independent providers, extends to multi-turn and RAG workflows, and survives rigorous statistical correction. The immediate implication is that a substantial portion of published research relying on API-based LLMs may contain non-reproducible results without the authors’ knowledge, a concern amplified by the growing use of LLMs in peer review[3], hypothesis generation[4], and agentic pipelines where non-determinism compounds at every step.

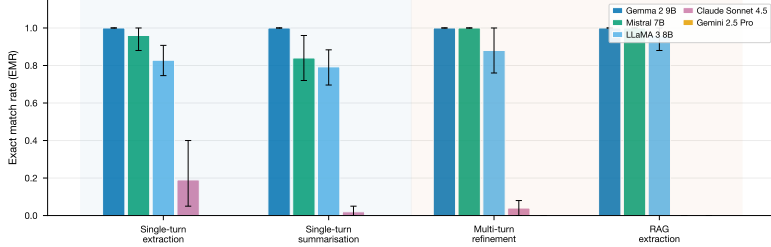


Fig. 2 Complex interaction regimes amplify the local–API reproducibility gap. EMR under greedy decoding ($C1, t = 0$) for five models across four scenarios: single-turn extraction, single-turn summarization, multi-turn refinement, and RAG extraction. Local models (Gemma 2, Mistral, LLaMA 3) maintain EMR ≥ 0.880 across all scenarios. Both API models (Claude Sonnet 4.5 and Gemini 2.5 Pro) exhibit near-zero EMR, with Claude achieving 0.000 for RAG (50 runs, zero exact matches). Error bars: 95% bootstrap CIs.

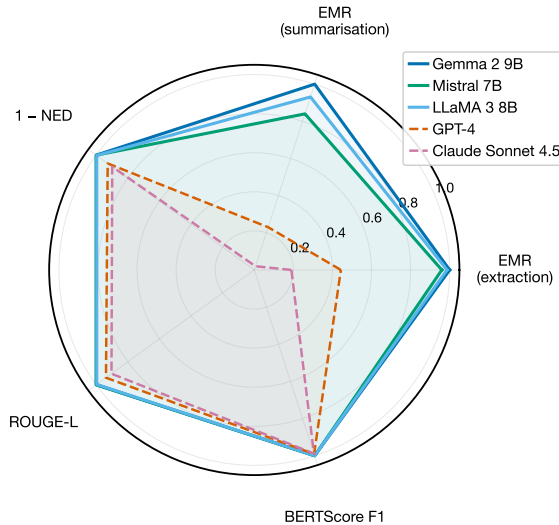


Fig. 3 API non-determinism is textual, not semantic. Three-level reproducibility profiles under greedy decoding. Local models (solid lines) occupy the outer region across all metrics. API models (dashed lines) show pronounced deficits in EMR and NED while maintaining BERTScore F1 > 0.97 (hidden non-determinism). Axes: EMR (extraction), EMR (summarization), 1–NED, ROUGE-L, BERTScore F1.

Prior work documented LLM non-determinism in isolated settings: inconsistent NLP benchmark outputs[27], failure of “deterministic” API settings[28], and non-deterministic code generation[29]. Our study advances beyond these observations by systematically comparing local versus API deployments across five providers, extending measurements to multi-turn and RAG workflows, and providing a causal attribution framework that distinguishes infrastructure complexity from cloud deployment.

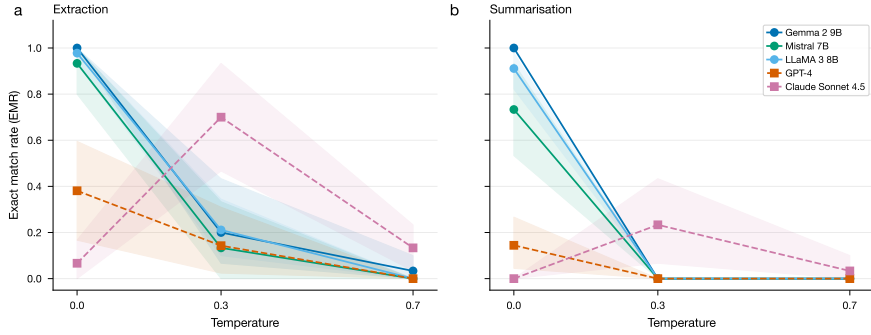


Fig. 4 Temperature paradox: greedy decoding is not greedy for API models. EMR versus temperature for five models (three local, two API). **a**, Extraction. **b**, Summarisation. Local models (solid lines) show the expected monotonic decline from near-perfect EMR at $t = 0$. API models (dashed lines) start from an already-low baseline. Claude Sonnet 4.5 (red dashed) exhibits a non-monotonic anomaly: extraction EMR *increases* from 0.067 at $t = 0$ to 0.700 at $t = 0.3$.

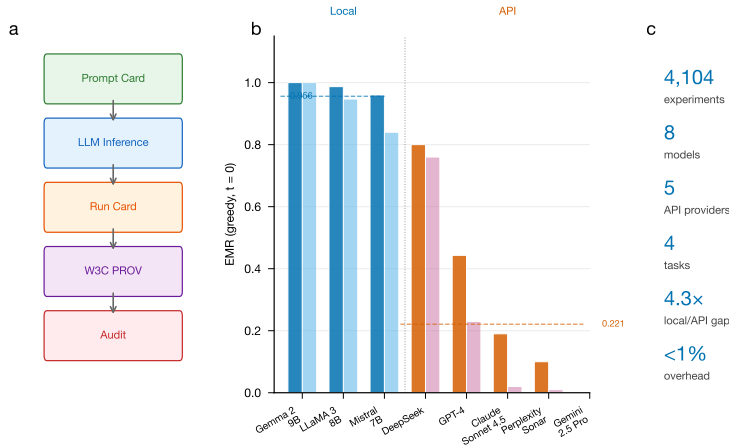


Fig. 5 Study overview and provenance protocol. **Left:** The provenance pipeline, from Prompt Card creation through Run Card logging and W3C PROV graph generation. **Centre:** EMR under greedy decoding for eight model deployments, illustrating the local-API reproducibility gap (local models green, EMR ≥ 0.840 ; API models red, EMR ≤ 0.800). **Right:** Key statistics: 4,104 experiments, 9 deployments, 7 execution environments, 4 tasks, <1% protocol overhead.

232 The Together AI quasi-isolation result provides a key mechanistic insight: because
 233 the same model architecture achieves near-local reproducibility via a different cloud
 234 API, the non-determinism observed in GPT-4, Claude, and Gemini is attributable to
 235 production serving complexity rather than cloud deployment itself. This suggests that
 236 reproducibility is a design choice that providers could address through deterministic
 237 execution modes or transparent documentation, rather than an inherent limitation.
 238 Documenting temperature zero as “deterministic” without disclosing infrastructure-
 239 level variation creates a false sense of reproducibility that may be more damaging than
 240 openly acknowledged stochasticity.

241 These findings also have regulatory implications. The EU AI Act[47] requires traceability for high-risk AI systems, and the NIST AI RMF[48] emphasizes transparency; 242 hidden non-determinism directly undermines both. Ethical guidelines for LLM use 243 in academic writing[20] similarly assume that documented configurations produce 244 predictable outputs, an assumption our results show to be unwarranted.

245 Although the semantic preservation we observe (BERTScore F1 > 0.97) suggests 246 that output quality is not corrupted, our field-level analysis shows that even “semantically 247 equivalent” outputs differ in conclusion-relevant fields; the 78% non-match rate 248 under “deterministic” settings represents a serious obstacle for regulatory submissions, 249 systematic reviews, and automated pipelines.

250 The provenance protocol we provide offers a practical path forward. Grounded in 251 W3C PROV[6] and adding less than 1% overhead (Extended Data Table 6), it creates 252 auditable records linking every output to its generation context. Its key property is 253 *differential diagnosis*: when all hashes match except the output hash, the divergence 254 is automatically attributed to the generation process, a result confirmed across all 255 4,104 runs (Supplementary Section S4). This implements what recent editorials have 256 advocated[7] and extends Model Cards[17] and Datasheets[18] to the inference layer. 257 We propose a minimum reporting standard (model identity, parameters, reproducibility 258 metrics, deployment mode, and output hashes) that our protocol automates at 259 negligible cost (Supplementary Information).

260 Our study has several limitations. It covers eight models across four tasks but 261 excludes code generation, mathematical reasoning, and creative writing. Input data 262 comprises 30 English-language AI/ML abstracts; other languages and domains may 263 show amplified effects. GPT-4 experiments used the gpt-4-0613 snapshot; newer 264 versions may differ, though the infrastructure-level mechanisms we identify are 265 general. Multi-turn and RAG experiments include only two API providers; extending 266 to others would strengthen generality. Sample sizes (10–30 abstracts per model) are 267 well-powered for the large observed effects ($d > 1.6$) but may miss subtler phenomena. 268

269 Conclusions

270 We have shown that the “deterministic” settings offered by major LLM API providers 271 do not deliver determinism in practice, creating a hidden reproducibility gap that 272 affects any study relying on API-served models. The gap spans five independent 273 providers, persists across multi-turn and retrieval-augmented generation workflows, 274 and remains invisible to users because semantic equivalence masks textual divergence. 275 By running the same open-weight model locally and via a cloud API, we isolate the 276 cause: production infrastructure complexity, not cloud deployment itself, drives the 277 non-determinism. Our lightweight provenance protocol, grounded in W3C PROV and 278 requiring less than 1% overhead, offers a practical mechanism for making this variation 279 visible, auditable, and attributable. Together with the minimum reporting standard 280 we propose, it provides an actionable path toward reproducible LLM-based research.

281 These findings raise a broader reliability concern. Large language models are no 282 longer confined to text generation; they are increasingly embedded in clinical decision 283 support, environmental monitoring, engineering design, automated data collection and

284 analysis, and other domains where outputs directly inform decisions with consequences
285 in the physical world. In such settings, the inability to reproduce or verify a model’s
286 output is not merely an academic inconvenience but a threat to the trustworthiness of
287 the systems that depend on it. Our results demonstrate that, without explicit prove-
288 nance tracking, the reliability of any LLM-based pipeline built on API inference cannot
289 be assumed; it must be measured, documented, and continuously monitored. As the
290 integration of AI into science and society accelerates, establishing the infrastructure
291 for verifiable and reproducible model outputs is not a technical nicety but a scientific
292 and societal necessity.

293 Methods

294 Protocol design

295 The provenance protocol addresses the question: what is the minimum metadata
296 needed per generative AI run to enable reproducibility assessment, auditing, and
297 provenance tracking? The FAIR principles[49] provide a foundation for data steward-
298 ship, yet no standard exists for documenting the full context of generative AI outputs.
299 Existing experiment-tracking tools such as MLflow[50] were designed for training
300 pipelines and numerical metrics, not for inference-time text-generation provenance.
301 Data leakage analysis across 17 ML fields[25] underscores the urgency of structured
302 documentation. It comprises four components.

303 **Prompt Cards** are versioned documentation artifacts capturing design rationale
304 and metadata for prompt templates, including SHA-256 hash, version, task category,
305 assumptions, limitations, and target models. The concept extends Model Cards[17]
306 and Datasheets for Datasets[18] to the prompt layer.

307 **Run Cards** capture the complete execution context of a single generative AI run
308 through 24 core fields organized into five groups: identification (run ID, prompt hash,
309 prompt text), model context (name, version, weights hash), parameters (temperature,
310 seed, decoding strategy, parameters hash), input/output (text and SHA-256 hashes),
311 and execution metadata (environment fingerprint, timestamps, duration, logging over-
312 head). For API models, optional extension fields capture provider-specific metadata:
313 API request ID, response headers, resolved model version, and a `seed_status` field
314 distinguishing between seeds that were “sent”, “logged-only” (recorded for protocol
315 parity but not transmitted, as with Claude), or “not-supported”.

316 **W3C PROV integration.** Each experimental group is translated into a PROV-
317 JSON document[6] expressing generation provenance as a directed graph of entities
318 (Prompt, InputText, ModelVersion, InferenceParameters, Output), activities (Run-
319 Generation), and agents (Researcher, SystemExecutor). The formal semantics of
320 PROV enable automated traversal and comparison, identifying the exact factor that
321 differs between non-identical outputs without custom parsing.

322 **Reproducibility checklist.** A 15-item checklist organized into four categories
323 (Prompt Documentation, Model and Environment, Execution and Output, Prove-
324 nance) enables self-assessment.

325 We formally define the protocol as a tuple $\mathcal{P} = (PC, RC, G, CL)$ and prove an *audit*
326 *completeness* property: for 10 defined audit questions, every question is answerable if

327 and only if all field groups are populated. An ablation analysis confirms *minimality*:
328 removing any field group renders at least one question unanswerable (Extended Data
329 Table 6).

330 Models and infrastructure

331 We evaluate nine model deployments across three paradigms.

332 **Local models** (Ollama v0.15.5, Apple M4, 24 GB unified memory, macOS 14.6,
333 Python 3.14.3): LLaMA 3 8B[30] (Q4_0), Mistral 7B[31] (Q4_0), Gemma 2 9B[32]
334 (Q4_0). Weights hashes recorded via the Ollama API.

335 **API-served models:** GPT-4 (gpt-4-0613)[33] via OpenAI API; Claude Son-
336 net 4.5 (claude-sonnet-4-5-20250929)[34] via Anthropic API (urllib, no SDK);
337 Gemini 2.5 Pro (gemini-2.5-pro-preview-05-06)[35] via Google AI Studio REST
338 API (urllib); DeepSeek Chat via OpenAI-compatible API; Perplexity Sonar via
339 Perplexity API.

340 **Quasi-isolation probe:** LLaMA 3 8B via Together AI (INT4, same architecture
341 as local, `meta-llama/Llama-3-8b-chat-hf`).

342 Tasks

343 Four tasks spanning the output-structure spectrum: **Task 1, Scientific summariza-**
344 **tion:** produce a three-sentence summary of a scientific abstract. **Task 2, Structured**
345 **extraction:** extract five fields (objective, method, key_result, model_or_system, bench-
346 mark) as JSON. **Task 3, Multi-turn refinement:** three-turn dialogue (extract,
347 receive feedback, refine). **Task 4, RAG extraction:** structured extraction with a
348 prepended retrieved context passage.

349 Input data

350 Thirty widely cited AI/ML abstracts (including Transformer, BERT, GPT-3, T5, and
351 Chain-of-Thought[36–40]), varying in length (74–227 words) and technical complexity.

352 Experimental conditions

353 Five conditions systematically vary reproducibility factors: **C1** (fixed seed, greedy):
354 $t = 0$, seed = 42, 5 repetitions; **C2** (variable seeds, greedy): $t = 0$, seeds = {42, 123,
355 456, 789, 1024}, 5 repetitions; **C3** (temperature sweep): $t \in \{0.0, 0.3, 0.7\}$, 3 repetitions
356 each. Tasks 1–2 under all conditions for five models with full coverage; Tasks 3–4
357 under C1 for local models, Claude, and Gemini. DeepSeek and Perplexity: C1 only
358 on Tasks 1–2. Together AI: C1 and C2 on Tasks 1–2. Grand total: 4,104 logged runs
359 across 9 deployments and 7 execution environments.

360 For API models, the seed parameter is advisory (OpenAI[12]), absent
361 (Anthropic), or empirically insufficient (Gemini); greedy decoding does not guarantee
362 determinism[29].

363 **Metrics**

364 **Exact Match Rate (EMR)**: fraction of all $\binom{n}{2}$ output pairs within a group that are
365 character-identical. **Normalised Edit Distance (NED)**: Levenshtein distance[42]
366 normalized by the longer string. **ROUGE-L F1**: longest common subsequence
367 overlap[41]. **BERTScore F1**: embedding-based semantic similarity[43]. For struc-
368 tured extraction, we additionally compute JSON validity rate, schema compliance, and
369 field-level accuracy. Protocol overhead: logging time (ms), storage (KB), and overhead
370 ratio (%).

371 **Statistical analysis**

372 All EMR values accompanied by 95% bootstrap confidence intervals (10,000 resamples,
373 percentile method, per-abstract EMR)[44]. Primary comparisons: Wilcoxon signed-
374 rank test (non-parametric) and paired *t*-test (parametric), with Holm–Bonferroni
375 correction across 68 hypothesis tests. Effect sizes: Cohen’s *d* (parametric) and Cliff’s
376 delta[45] (non-parametric). Power analysis confirms >0.95 for all primary comparisons
377 at the observed effect sizes (*d* > 1.6)[46]. Balanced 10-abstract subsample analysis
378 confirms robustness (local EMR = 0.953 vs. API EMR = 0.304, 3.1×).

379 **Sources of non-determinism in distributed inference**

380 Six well-documented mechanisms can independently produce non-deterministic out-
381 puts under greedy decoding in distributed GPU inference: (1) non-associative
382 floating-point arithmetic[15]; (2) mixed-precision accumulation in BF16/FP16[11];
383 (3) tensor parallelism and all-reduce non-determinism[8]; (4) FlashAttention kernel
384 non-determinism[16]; (5) dynamic batching and continuous request scheduling[10];
385 (6) speculative decoding[9]. Our single-GPU local deployment eliminates mechanisms
386 (3)–(6) and GGML Q4 integer arithmetic mitigates (2), explaining near-perfect local
387 reproducibility as a predicted consequence.

388 **Protocol overhead**

389 The protocol adds <1% overhead across all models profiled: mean logging time 21–
390 30 ms versus inference latency of 4–182 s. Storage: ~4 KB per run (16 MB total for
391 4,104 runs). The overhead is consistent across local and API deployment.

392 **Reporting summary**

393 Further information on research design is available in the Nature Portfolio Reporting
394 Summary linked to this article.

395 **Data availability.** All 4,104 run records (JSON), PROV-JSON provenance
396 documents, Run Cards, Prompt Cards, input data (30 abstracts with DOIs),
397 and generated figures are publicly available at <https://github.com/Roverlucas/genai-reproducibility-protocol> under CC-BY 4.0 license. Source data are provided with
398 this paper.

400 **Code availability.** The reference implementation of the provenance protocol, all
401 analysis scripts, and figure-generation code are publicly available at <https://github.com/Roverlucas/genai-reproducibility-protocol> under MIT License.
402

403 **Supplementary information.** The Supplementary Information (single PDF) con-
404 tains: (S1) Full prompts for all four tasks; (S2) All 30 abstracts with DOIs;
405 (S3) Retrieved contexts for RAG experiments; (S4) API payload documentation for
406 all nine deployments; (S5) Protocol comparison table (our protocol vs. MLflow, W&B,
407 DVC, OpenAI Eval, LangSmith); (S6) Ablation study: protocol minimality verifi-
408 cation (10 audit questions \times 8 field groups); (S7) Chat-format control experiment
409 (200 runs); (S8) 15-item reproducibility checklist; (S9) Statistical test results (full
410 Holm–Bonferroni table, 68 tests); (S10) Environment and provenance transparency
411 documentation.

412 **Acknowledgements.** This work was supported by UTFPR—Universidade Tec-
413 nológica Federal do Paraná.

414 **Declarations**

- 415 • **Funding:** This research received no specific grant from any funding agency in the
416 public, commercial, or not-for-profit sectors.
- 417 • **Author contributions:** L.R. conceived the study, designed the protocol, developed
418 the software, conducted all experiments and analyses, and wrote the manuscript.
419 E.T.B. contributed to experimental design and data analysis. A.T.d.A. contributed
420 to methodology design and statistical analysis. Y.d.S.T. supervised the research,
421 contributed to methodology design, and reviewed the manuscript.
- 422 • **Competing interests:** The authors declare no competing interests.
- 423 • **Correspondence:** Correspondence and requests for materials should be addressed
424 to Lucas Rover (lucasrover@utfpr.edu.br).

425 **Extended Data**

426 **Extended Data Table 1.** Full three-level reproducibility assessment (EMR, NED,
427 ROUGE-L, BERTScore F1) for all models under greedy decoding.

428 **Extended Data Table 2.** API versus local summary statistics with Cliff’s delta
429 effect sizes and bootstrap confidence intervals on the EMR ratio.

430 **Extended Data Table 3.** Temperature sweep: EMR at $t \in \{0.0, 0.3, 0.7\}$ for five
431 models.

432 **Extended Data Table 4.** Balanced 10-abstract subsample robustness analysis.

433 **Extended Data Table 5.** Warm-up analysis: cold-start effect characterization.

434 **Extended Data Table 6.** Protocol overhead and ablation matrix (protocol mini-
435 mality verification).

436 **Extended Data Table 7.** Conclusion divergence analysis: GPT-4 field-level differ-
437 ences.

438 **Extended Data Fig. 1.** Normalised Edit Distance comparison across all models and
439 tasks.

440 **Extended Data Fig. 2.** Run Card schema and W3C PROV graph example for a
441 single experimental group.

442 References

- 443 [1] Singhal, K. *et al.* Large language models encode clinical knowledge. *Nature* **620**,
444 172–180 (2023).
- 445 [2] Thirunavukarasu, A. J. *et al.* Large language models in medicine. *Nat. Med.* **29**,
446 1930–1940 (2023).
- 447 [3] Thakkar, N. *et al.* A large-scale randomized study of large language model
448 feedback in peer review. *Nat. Mach. Intell.* **8**, online (2026).
- 449 [4] Xin, H., Kitchin, J. R. & Kulik, H. J. Towards agentic science for advancing
450 scientific discovery. *Nat. Mach. Intell.* **7**, 1373–1375 (2025).
- 451 [5] Multi-agent AI systems need transparency [editorial]. *Nat. Mach. Intell.* **8**, 1
452 (2026).
- 453 [6] Moreau, L. & Missier, P. PROV-DM: The PROV Data Model. W3C Recommen-
454 dation (2013); <https://www.w3.org/TR/prov-dm/>.
- 455 [7] What is in your LLM-based framework? [editorial]. *Nat. Mach. Intell.* **6**, 845
456 (2024).
- 457 [8] Shoeybi, M. *et al.* Megatron-LM: training multi-billion parameter language
458 models using model parallelism. Preprint at <https://arxiv.org/abs/1909.08053>
459 (2019).
- 460 [9] Leviathan, Y., Kalman, M. & Matias, Y. Fast inference from transformers via
461 speculative decoding. In *Proc. ICML* Vol. 202, 19274–19286 (PMLR, 2023).
- 462 [10] Kwon, W. *et al.* Efficient memory management for large language model serving
463 with PagedAttention. In *Proc. 29th ACM SOSP* (2023).
- 464 [11] Yuan, J. *et al.* Understanding and mitigating numerical sources of nondetermin-
465 ism in LLM inference. In *Advances in NeurIPS* Vol. 38 (2025).
- 466 [12] OpenAI. API Reference: Create Chat Completion—Seed Parameter. <https://platform.openai.com/docs/api-reference/chat/create> (2024).
- 468 [13] Kumar, A. *et al.* When large language models are reliable for judging empathic
469 communication. *Nat. Mach. Intell.* **8**, 173–185 (2026).

- 470 [14] Serapio-García, G. *et al.* A psychometric framework for evaluating and shap-
471 ing personality traits in large language models. *Nat. Mach. Intell.* **7**, 1954–1968
472 (2025).
- 473 [15] Higham, N. J. *Accuracy and Stability of Numerical Algorithms* 2nd edn (SIAM,
474 2002).
- 475 [16] Dao, T. *et al.* FlashAttention: fast and memory-efficient exact attention with
476 IO-awareness. In *Advances in NeurIPS* Vol. 35 (2022).
- 477 [17] Mitchell, M. *et al.* Model cards for model reporting. In *Proc. FAccT* 220–229
478 (ACM, 2019).
- 479 [18] Gebru, T. *et al.* Datasheets for datasets. *Commun. ACM* **64**, 86–92 (2021).
- 480 [19] Gundersen, O. E., Helmert, M. & Hoos, H. H. Improving reproducibility in AI
481 research: four mechanisms adopted by JAIR. *J. Artif. Intell. Res.* **81**, 1019–1041
482 (2024).
- 483 [20] Porsdam Mann, S. *et al.* Guidelines for ethical use and acknowledgement of large
484 language models in academic writing. *Nat. Mach. Intell.* **6**, 1272–1274 (2024).
- 485 [21] Baker, M. 1,500 scientists lift the lid on reproducibility. *Nature* **533**, 452–454
486 (2016).
- 487 [22] Hutson, M. Artificial intelligence faces reproducibility crisis. *Science* **359**, 725–726
488 (2018).
- 489 [23] Gundersen, O. E. & Kjensmo, S. State of the art: reproducibility in artificial
490 intelligence. *Proc. AAAI* **32**, 1644–1651 (2018).
- 491 [24] Ball, P. Is AI leading to a reproducibility crisis in science? *Nature* **624**, 22–25
492 (2023).
- 493 [25] Kapoor, S. & Narayanan, A. Leakage and the reproducibility crisis in machine-
494 learning-based science. *Patterns* **4**, 100804 (2023).
- 495 [26] Birhane, A. *et al.* Science in the age of large language models. *Nat. Rev. Phys.* **5**,
496 277–280 (2023).
- 497 [27] Chen, Y. *et al.* On the reproducibility of ChatGPT in NLP tasks. Preprint at
498 <https://arxiv.org/abs/2304.02554> (2023).
- 499 [28] Atil, B. *et al.* Non-determinism of “deterministic” LLM settings. Preprint at
500 <https://arxiv.org/abs/2408.04667> (2024).
- 501 [29] Ouyang, S. *et al.* An empirical study of the non-determinism of ChatGPT in code
502 generation. *ACM Trans. Softw. Eng. Methodol.* **34**, 1–28 (2024).

- 503 [30] Grattafiori, A. *et al.* The LLaMA 3 herd of models. Preprint at <https://arxiv.org/abs/2407.21783> (2024).
- 504
- 505 [31] Jiang, A. Q. *et al.* Mistral 7B. Preprint at <https://arxiv.org/abs/2310.06825> (2023).
- 506
- 507 [32] Gemma Team *et al.* Gemma 2: improving open language models at a practical size. Preprint at <https://arxiv.org/abs/2408.00118> (2024).
- 508
- 509 [33] Achiam, J. *et al.* GPT-4 technical report. Preprint at <https://arxiv.org/abs/2303.08774> (2023).
- 510
- 511 [34] Anthropic. The Claude Model Family. <https://www.anthropic.com/clause> (2024).
- 512
- 513 [35] Reid, M. *et al.* Gemini 1.5: unlocking multimodal understanding across millions of tokens of context. Preprint at <https://arxiv.org/abs/2403.05530> (2024).
- 514
- 515 [36] Vaswani, A. *et al.* Attention is all you need. In *Advances in NeurIPS* Vol. 30 (2017).
- 516
- 517 [37] Devlin, J. *et al.* BERT: pre-training of deep bidirectional transformers for language understanding. In *Proc. NAACL* 4171–4186 (ACL, 2019).
- 518
- 519 [38] Brown, T. *et al.* Language models are few-shot learners. In *Advances in NeurIPS* Vol. 33, 1877–1901 (2020).
- 520
- 521 [39] Raffel, C. *et al.* Exploring the limits of transfer learning with a unified text-to-text transformer. *J. Mach. Learn. Res.* **21**, 1–67 (2020).
- 522
- 523 [40] Wei, J. *et al.* Chain-of-thought prompting elicits reasoning in large language models. In *Advances in NeurIPS* Vol. 35, 24824–24837 (2022).
- 524
- 525 [41] Lin, C.-Y. ROUGE: a package for automatic evaluation of summaries. In *Proc. ACL Workshop on Text Summarization* 74–81 (2004).
- 526
- 527 [42] Levenshtein, V. I. Binary codes capable of correcting deletions, insertions, and reversals. *Sov. Phys. Dokl.* **10**, 707–710 (1966).
- 528
- 529 [43] Zhang, T. *et al.* BERTScore: evaluating text generation with BERT. In *Proc. ICLR* (2020).
- 530
- 531 [44] Efron, B. & Tibshirani, R. J. *An Introduction to the Bootstrap* (Chapman & Hall/CRC, 1993).
- 532
- 533 [45] Romano, J. *et al.* Appropriate statistics for ordinal level data. In *Annual Meeting of the Florida Association of Institutional Research* (2006).
- 534

- 535 [46] Cohen, J. *Statistical Power Analysis for the Behavioral Sciences* 2nd edn
536 (Erlbaum, 1988).
- 537 [47] European Parliament. Regulation (EU) 2024/1689 laying down harmonised rules
538 on artificial intelligence (AI Act) (2024).
- 539 [48] NIST. Artificial Intelligence Risk Management Framework (AI RMF 1.0). U.S.
540 Department of Commerce (2023).
- 541 [49] Wilkinson, M. D. *et al.* The FAIR guiding principles for scientific data manage-
542 ment and stewardship. *Sci. Data* **3**, 160018 (2016).
- 543 [50] Zaharia, M. *et al.* Accelerating the machine learning lifecycle with MLflow. *IEEE*
544 *Data Eng. Bull.* **41**, 39–45 (2018).